TÜBİTAK

Turkish Journal of Botany

http://journals.tubitak.gov.tr/botany/

Research Article

Turk J Bot
(2015) 39: 472-486

doi:10.3906/bot-1406-87

Phylogeny and systematics of the western Mediterranean *Vella pseudocytisus-V. aspera* complex (Brassicaceae)

Violeta I. SIMÓN-PORCAR[1,2,*], Ernesto PÉREZ-COLLAZOS[1,*,], Pilar CATALÁN[1,3]**

[1]Department of Agricultural and Environmental Sciences, Polytechnic School of Huesca, University of Zaragoza, Huesca, Spain
[2]Biological and Environmental Sciences, School of Natural Sciences, University of Stirling, Stirling, UK
[3]Department of Botany, Institute of Biology, Tomsk State University, Tomsk, Russia

Received: 30.06.2014 • **Accepted:** 15.12.2014 • **Published Online:** 04.05.2015 • **Printed:** 29.05.2015

Abstract: The evolution and taxonomy of the core members of subtribe Vellinae (Brassicaceae), comprising *Vella aspera*, *V. bourgeana*, and *V. pseudocytisus*, is still poorly known. We reconstructed the evolutionary relationships among these taxa and other Vellinae and close Brassicaceae using nuclear ITS and plastid *trn*TF phylogenies, and analyzed the phenotypic traits that differentiate the infraspecific ranks of *V. pseudocytisus*. Our phylogenetic analyses show: i) an early divergence of *Succowia* within the Brassiceae-Sisymbrieae sensu lato clade; ii) the nested positions of *Vella bourgeana* (syn. *Euzomodendron bourgaeanum*) and *V. aspera* (syn. *Boleum asperum*) within the *Vella* clade; and iii) the split of 5 lineages within the *V. pseudocytisus* clade (NW African subspecies *glabrata* 2x; SE Spain subspecies *pseudocytisus* 2x; C Spain subspecies *pseudocytisus* 4x; NE Spain subspecies *paui* 4x Alfambra Valley; and NE Spain subspecies *paui* 4x Turia Valley). Phenotypic traits support the differentiation of the diploid and tetraploid cytotypes of *V. pseudocytisus* subsp. *pseudocytisus*. Our data support the separation of *Succowia* from the Vellinae and the erection of a new subspecies within *V. pseudocytisus* (*Vella pseudocytisus* subsp. *orcensis* subsp. nov.). They also corroborate the inclusion of *Boleum* and *Euzomodendron* within *Vella*.

Key words: Bayesian and parsimony phylogenies, Bayesian relaxed-clock dating, plastid and nuclear DNA sequences (ITS, *trn*TL, *trn*LF), taxonomy, Vellinae

1. Introduction

Brassicaceae is one of the most diverse lineages of angiosperms, comprising approximately 321–338 genera and 3660–3709 species (Warwick et al., 2006; Al-Shehbaz, 2012). The family was traditionally separated into 10–19 different tribes according to fruit shape and the position of the embryo and cotyledons, each containing different subtribes (Janchen, 1942). However, recent classifications based on molecular phylogenies have recognized a larger number of tribes (25, Beilstein et al., 2008; 49, Al-Shehbaz, 2012); additionally, the tribal and subtribal arrangements vary according to the outputs of the different molecular phylogenetic studies (Beilstein et al., 2008, 2010; Couvreur et al., 2010; Al-Shehbaz, 2012; Arias et al., 2014). The subtribe Vellinae, formerly classified within the tribe Brassiceae, has been the subject of systematic discussion for decades (Schulz, 1936; Gómez-Campo, 1981; Warwick and Black, 1994; Warwick and Al-Shehbaz, 1998; Crespo et al., 2000). According to the molecular and morphological study of Crespo et al. (2000), the Vellinae comprise the annual herbaceous genera *Succowia* (L.) Medik. (1 species) and *Carrichtera* (L.) DC. (1 species), which are widespread in the dry steppe habitats of the Mediterranean and the Irano-Turanian areas, and the narrow endemic perennial woody genera *Euzomodendron* Coss. (1 species) and *Vella* L. (7 species including *Boleum* Desv), which grow in continental climate sites of central and southern Spain and northern Morocco and Algeria. The taxonomy of the core subtribe Vellinae members (*Boleum*, *Euzomodendron*, *Vella*) has been controversial (Gómez-Campo, 1981; Warwick and Black, 1994; Warwick and Al-Shehbaz, 1998; Crespo et al., 2000; Al-Shehbaz, 2012). Warwick and Al-Shehbaz (1998), using chloroplast DNA restriction site variation, cytology, and morphological data, subsumed the 3 genera within *Vella*, whereas Crespo et al. (2000), using ITS and morphological data, retained *Euzomodendron*

* These two authors contributed equally to this work.
** Correspondence: ernextop@unizar.es

as an independent genus but included the monotypic *Boleum* in *Vella* (*Vella aspera*), as originally described by Persoon (1806). The taxonomic treatment adopted in this study includes *Boleum* and *Euzomodendron* within *Vella*, following Al-Shehbaz (2012). *Vella aspera* (syn. *Boleum asperum*), *V. bourgeana* (syn. *Euzomodendron bourgaeanum*), and *V. pseudocytisus* are closely related taxa that share not only their perennial habit but also some morphological traits, such as connate inner stamens and navicular fruit valves (Crespo et al., 2000). The 3 species also show a common chromosome base number of x = 17; however, different ploidy levels, ranging from diploid to hexaploid, occur across taxa and geographical ranges (e.g., *Vella bourgeana*, 2n = 34 (2x); *V. pseudocytisus*, 2n = 34 (2x) and 2n = 68 (4x); *V. aspera*, 2n = 102 (6x); Gómez-Campo, 1981; Blanca et al., 1999). The most widely distributed species of the *Vella pseudocytisus-V. aspera* complex is *V. pseudocytisus* L., a spineless plant characterized by shortly spatulate leaves with obtuse apices and elongated fruit racemes (Gómez-Campo, 1993). The species includes 3 subspecies, taxonomically differentiated by the hairiness of the leaves, the inflorescence axes, and the fruits (Gómez-Campo, 1981). They show disjunct distributions in the Magrebian region and in the southern, central, and northeastern regions of Spain (Gómez-Campo, 1981, 1993; Crespo et al., 2000; Figure 1). *Vella pseudocytisus* subsp. *pseudocytisus* is an Iberian endemic distributed in 2 separate ranges: central Spain (Madrid and Toledo), with populations containing tetraploid individuals (2n = 68), and SE Spain (Granada), with populations containing diploid individuals (2n = 34; Gómez-Campo, 1981, 1993; Blanca et al., 1999). *Vella pseudocytisus* subsp. *glabrata* Greuter (syn. *Vella pseudocytisus* subsp. *glabrescens* (Cosson) Litard. & Maire) is a diploid plant (2n = 34) that occurs in 3 northwestern African ranges, in the Atlas (Morocco) and Tell-Atlas (Morocco, Algeria) mountains (Gómez-Campo, 1981). The third subspecies, *Vella pseudocytisus* subsp. *paui* Gómez-Campo (=*Vella paui* Pau nom. nudum), is a tetraploid taxon (2n = 68) distributed in a narrow range in NE Spain (Teruel Province) (Gómez-Campo, 1981; Pérez-Collazos and Catalán, 2006). In contrast to *Vella pseudocytisus*, *V. aspera* is a narrow endemic hexaploid species that shows a restricted distribution area of 140 km^2 in NE Spain (middle Ebro Valley region) (Guzmán et al., 2000; Pérez-Collazos et al., 2008; Figure 1).

Despite their disjunct distribution, the 3 subspecies of *Vella pseudocytisus* and *V. aspera* share similar climate and edaphic conditions, growing in Miocene gypsum and carbonate-rich soils in places characterized by extreme continental dry weather (Gómez-Campo, 1981). Within *Vella pseudocytisus*, range differences in ploidy level and cryptic morphological traits (Gómez-Campo, 1981; Blanca et al., 1999) and in molecular spatial structure (Pérez-Collazos, 2005) suggest the potential existence of microspeciation processes within the complex. In addition, the intraspecific taxonomic circumscriptions within *Vella pseudocytisus* s.l. are in need of a deep systematic revision.

In this study, we aimed to reconstruct the evolutionary relationships among the 5 groups (4 taxa, 5 geographic range cytotypes; Figure 1) of the *Vella pseudocytisus-V. aspera* complex and update their taxonomic treatment. Our objective was to reconstruct the phylogenetic relationships across the geographic ranges and cytotypes of the complex. For this purpose, we applied parsimony and Bayesian inference methods based on DNA sequences from the biparentally inherited nuclear ribosomal ITS locus, a genomic region widely used in phylogenetic reconstructions of angiosperms (Baldwin et al., 1995), and from the maternally inherited chloroplast *trn*TL and *trn*LF loci, frequently used in phylogenetic studies of plant species with hybrid origin (Jiménez et al., 2005). We also estimated the times of divergence of the lineages using Bayesian relaxed-clock methods to frame the spatiotemporal history of the group in the western Mediterranean area. The taxonomic study was based on statistical analysis of selected quantitative and qualitative traits across subspecies and cytotypes of *Vella pseudocytisus* s.l., aiming to disentangle the potential existence of new intraspecific taxa within this taxon.

2. Materials and methods

2.1. Sampling, DNA isolation, PCR amplification, and sequencing

Sampled material for molecular analysis included representatives of *Vella pseudocytisus* and *V. aspera* collected across the entire geographical distribution range of each taxon. Fresh leaves of 1–3 individuals from 22 populations of the taxa were sampled, rendering a total of 64 samples (Table 1; Figure 1). All individual samples were collected in the field, except those of *Vella pseudocytisus* subsp. *glabrata*, which were obtained from Moroccan seeds stored at the Spanish INIA germplasm bank. The samples were germinated in moist paper in petri dishes and grown under standard greenhouse conditions. Additionally, samples from other representatives of Vellinae (*Carrichtera annua*, *Succowia balearica*, *Vella bourgeana*, *V. lucentina*, *V. marei*, and *V. spinosa*) and from another close Brassicaceae (*Diplotaxis erucoides*) were collected in the field, rendering 15 extra samples (Table 1).

Silica gel-dried leaves were ground into powder using liquid nitrogen. Thirty milligrams of each sample were used for DNA extraction following the standard protocol described by Doyle and Doyle (1990). DNA quality and concentration was estimated in 1% agarose gels. We performed polymerase chain reaction (PCR) separately for the chloroplast regions *trn*TL and *trn*LF, using primers

Table 1. Origins of the studied samples of the *Vella pseudocytisus-V. aspera* complex and other Brassicaceae taxa used in the ITS and *trn*TL-LF phylogenetic analysis. Ploidy, Lat: latitude, Long: longitude, Pop: population code, N: number of individuals sampled, na: data not available.

Taxon	Locality	Ploidy	Lat	Long	Pop	N
Vella pseudocytisus (subsp.)-*V.aspera* complex						
subsp. *paui*	Spain: Teruel; Alfambra Valley: Villalba	4x	40.43	–1.05	VP01	3
subsp. *paui*	Spain: Teruel; Alfambra Valley: Villalba Baja	4x	40.42	–1.07	VP02	3
subsp. *paui*	Spain: Teruel; Turia Valley: Villel 1	4x	40.23	–1.15	VP03	3
subsp. *paui*	Spain: Teruel; Turia Valley: Villel 2	4x	40.25	–1.12	VP04	3
subsp. *paui*	Spain: Teruel; Turia Valley: Villastar 1	4x	40.22	–1.02	VP05	3
subsp. *paui*	Spain: Teruel; Turia Valley: Villastar 2	4x	40.23	–1.13	VP06	3
subsp. *pseudocytisus*	Spain: Granada; Puebla Don Fabrique	2x	37.83	–2.33	VP07	3
subsp. *pseudocytisus*	Spain: Granada; Orce 1	2x	37.70	–2.40	VP08	3
subsp. *pseudocytisus*	Spain: Granada; Orce 2	2x	37.75	–2.37	VP09	3
subsp. *pseudocytisus*	Spain: Toledo; Ontigola	4x	40.00	–3.57	VP10	3
subsp. *pseudocytisus*	Spain: Madrid; Aranjuez 1	4x	40.02	–3.55	VP11	3
subsp. *pseudocytisus*	Spain: Madrid; Aranjuez 2	4x	40.03	–3.55	VP12	3
subsp. *glabrata*	Morocco: Atlas; Midelt 1	2x	32.67	–4.73	VP13	3
subsp. *glabrata*	Morocco: Atlas; Midelt 2	2x	32.62	–4.75	VP14	1
V. aspera	Spain: Huesca; C Ebro Valley: Valcuerna 1	6x	41.47	0.17	VA01	3
V. aspera	Spain: Huesca; C Ebro Valley: Valcuerna 2	6x	41.47	0.00	VA02	3
V. aspera	Spain: Zaragoza; S Ebro Valley: Caspe 1	6x	41.20	0.17	VA03	3
V. aspera	Spain: Zaragoza; S Ebro Valley: Caspe 2	6x	41.18	0.10	VA04	3
V. aspera	Spain: Zaragoza; S Ebro Valley: Caspe 3	6x	41.17	0.01	VA05	3
V. aspera	Spain: Zaragoza; S Ebro Valley: Caspe 4	6x	41.23	0.02	VA06	3
V. aspera	Spain: Zaragoza; NW Ebro Valley: Monegrillo	6x	41.62	–0.45	VA07	3
V. aspera	Spain: Huesca; NW Ebro Valley: Castelflorite	6x	41.80	0.02	VA08	3
Other Vellinae						
Carrichtera annua	Spain: Almería; Cabo de Gata 1	2x	36.77	–2.23	CA01	1
Carrichtera annua	Spain: Almería; Cabo de Gata 2	2x	36.78	–2.25	CA02	1
Carrichtera annua	Spain: Almería; Paterna	2x	na	Na	CA03	1
Carrichtera annua	Spain: Tarragona; Xerta	2x	40.90	0.47	CA04	1
Succowia balearica	Spain: Barcelona; Bruguers	2x	41.32	1.95	SB01	1
Vella bourgeana	Spain: Almería; Tabernas 1	2x	37.03	–2.42	EB01	1
Vella bourgeana	Spain: Almería; Tabernas 2	2x	37.15	–2.68	EB02	1
Vella lucentina	Spain: Alicante; Alicante 1	2x	38.48	–0.57	VL01	1
Vella lucentina	Spain: Alicante; Alicante 2	2x	na	Na	VL02	1
Vella marei	Morocco: Atlas; Midelt	4x	na	Na	VM01	1
Vella spinosa	Spain: Alicante; Benissa 1	2x	38.73	0.45	VS01	1
Vella spinosa	Spain: Alicante; Benissa 2	2x	40.05	0.51	VS02	1
Vella spinosa	Spain: Alicante; Benissa 3	2x	na	Na	VS03	1
Sisymbrieae						
Diplotaxis erucoides	Spain: Castellón; Zucaina	2x	40.12	0.43	DE01	1
Diplotaxis erucoides	France: Dordogne; Vergt	2x	45.04	0.76	DE02	1

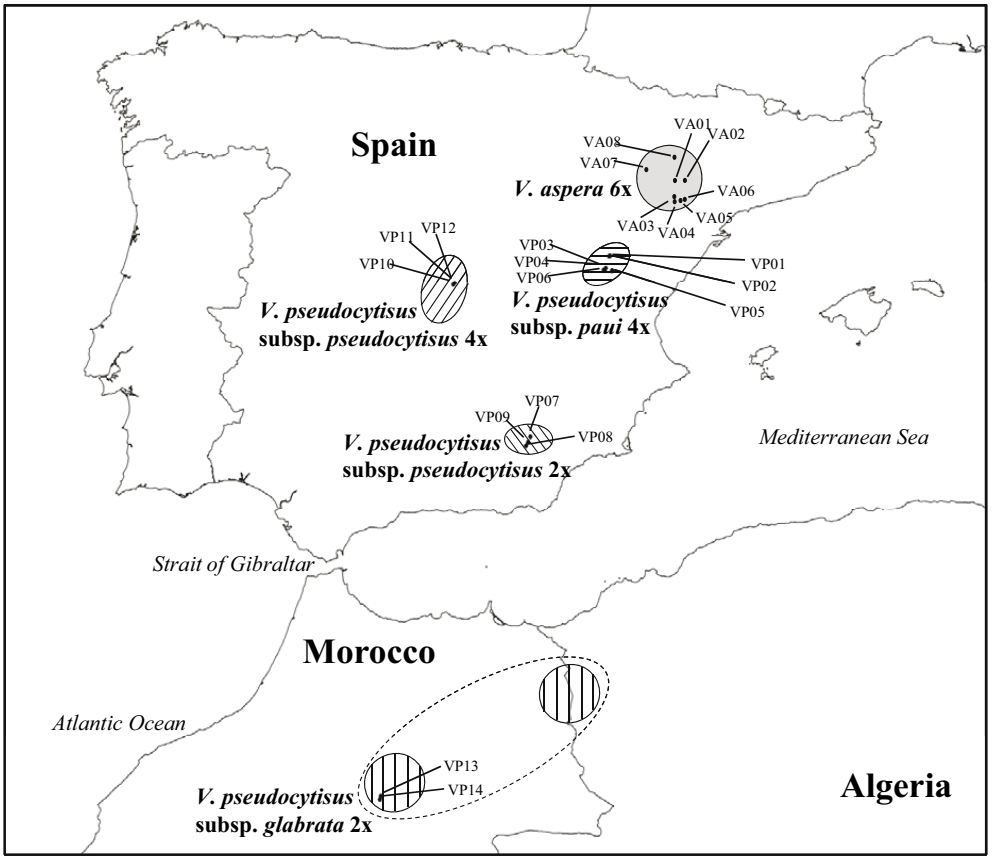

Figure 1. Geographical distribution of the *Vella pseudocytisus*-*V. aspera* complex taxa and cytotypes in the western Mediterranean region: *V. pseudocytisus* subspecies *glabrata* 2x (Mahgreb, N Morocco, and Algeria, vertical bars), *pseudocytisus* 2x (SE Spain, left diagonal bars), *pseudocytisus* 4x (C Spain, right diagonal bars), *paui* 4x (NE Spain, horizontal bars), and *V. aspera* 6x (NE Spain, middle Ebro Valley (Monegros), gray). The localities of studied populations are indicated on the map. Population codes correspond to those indicated in Table 1.

a and b, and c and f, respectively (Taberlet et al., 1991), and the ribosomal nuclear region ITS, using primers ITS1 and ITS4 (White et al., 1990). The PCR cocktail to amplify the *trn*TL and ITS regions consisted of 5 µL of buffer (10X), 5 µL of $MgCl_2$ (50 mM), 2 µL of dNTPs (10 mM), 1.5 µL of primers (20 µM), 0.5 µL of Taq (5 U/µL), 32.5 µL of Milli-Q water, and 2 µL of DNA. For the *trn*LF region, the mix consisted of 5 µL of buffer (10X), 2.5 µL of $MgCl_2$ (50 mM), 0.5 µL of dNTPs (10 mM), 0.3 µL of primers (20 µM), 0.3 µL of Taq (5 U/µL), 40.1 µL of Milli-Q water, and 1 µL of DNA. The PCR thermocycler program for all the regions was initiated for 4 min at 94 °C, followed by 35 cycles of 60 s at 94 °C, 60 s at 52 °C, and 150 s at 72 °C, with a final extension of 7 min at 72 °C. PCR products were purified using the QIAquick PCR purification kit (QIAGEN, the Netherlands) and sequencing was performed by Macrogen, using an ABI PRISM 373 sequencer (Macrogen, South Korea).

2.2. Phylogenetic analysis

Forward and reverse sequences were assembled and edited using Sequencher ver. 4.2.2 (Gene Codes Corporation, USA). In order to increase the taxonomic sampling of other Vellinae and Brassicaceae representatives, 25 additional DNA sequences from 15 taxa were downloaded from GenBank and included in the analyses (Table S1). Multiple alignments of the 3 independent datasets were conducted using MEGA 5.2 (Tamura et al., 2011). DNA insertions and deletions (indels) in the alignments were coded as binary characters, appended to the sequence matrix for each gene, and used in the parsimony analyses.

We performed separate and combined phylogenetic analyses for the 3 ITS, *trn*TL, and *trn*LF datasets using maximum parsimony and Bayesian inference-based methods. *Thlaspi perfoliatum* (Thlaspieae) was selected as the outgroup (Muller, 1981) and was used to root the trees. A concatenated plastid (cpDNA) dataset was constructed for

taxa with common sequences from the separate *trn*TL and *trn*LF datasets. Based on the topological congruence of the separate plastid (cpDNA) and nuclear ITS topologies (see Section 3) and the nonsignificant $P < 0.01$ results of the ILD test ($P = 0.02$) conducted in PAUP* ver. 4.0.beta (Swofford, 2002), the 2 datasets were united into a single data matrix for further combined analysis of the study group, using separate models for the plastid and the nuclear sequence data. Maximum parsimony searches were performed with PAUP* using a heuristic search protocol with 100 replicates of random-addition-taxa and tree bisection-reconnection (TBR) branch swapping. Clade robustness was assessed by a 1000-replicate bootstrap analysis using the same parameters as the original search. Bayesian analyses were performed using MrBayes v3.1 (Huelsenbeck and Ronquist, 2001). The GTR + I + G model was selected as the optimal nucleotide substitution model of each dataset according to the hierarchical likelihood ratio test (hLRT), the Akaike information criterion (AIC), and the Bayesian information criterion (BIC) implemented in jModelTest 2 (Guindon and Gascuel, 2003; Darriba et al., 2012), and was then subsequently imposed on all the independent and combined searches. Bayesian analysis consisted of 2 parallel Markov chain Monte Carlo (MCMC) runs of 4 chains performed with a length of 5×10^6 generations and a variable burn-in of 60,000–100,000 generations. To calculate the burn-in of each dataset, a Bayesian analysis was run for 1×10^6 generations, sampling every 100 generations, and the log of maximum likelihood was represented against the number of generations in order to visualize the number of generations necessary to reach a stable value (Huelsenbeck and Ronquist, 2001; Leaché and Reeder, 2002). A 50% majority rule consensus tree with the Bayesian posterior probability support (PPS) for each branch was calculated for each analysis.

2.3. Dating analysis

Like most angiosperms, the Brassicaceae have a poor record of young fossils (Beilstein et al., 2010; Couvreur et al., 2010). Most of the age estimations for the early diverging Brassicaceae lineages were calibrated using the Turonian fossil *Dressiantha* (ca. 85 Ma; Gandolfo et al., 1997). However, no fossils have been found for the species of the *Vella pseudocytisus-V. aspera* complex. In this study, we used the Oligocene fossil *Thlaspi primaevum* (Brassicaceae) from the Ruby Basin flora of southwestern Montana (30.8–29.2 Ma; Muller, 1981) to calibrate the nodal age of the common ancestor of the ingroup and the outgroup Thlaspieae samples. Our molecular dating analysis was performed on the well-resolved nuclear ITS phylogeny, using a Bayesian relaxed-clock approach implemented in BEAST v.1.7.4 (Drummond and Rambaut, 2007). Other parameters of the BEAST search included the GTR + G + I nucleotide substitution model, a birth-death evolutionary process model with random start to infer the trees' topologies, a lognormal calibration for the node of the most recent common ancestor (MRCA) of Thlaspieae + ingroup clade set to 30 ± 0.5 Ma, and an angiosperm molecular evolutionary rate of mutation of 1^{-4} to 1^{-1}, allowing BEAST to infer the topology, the branch lengths, and the nodal dates. The BEAST MCMC chain length analysis was run for 10×10^6 generations, saving data every 1000 generations and producing 10,000 estimates of dates and trees. Convergence statistics for each prior parameter were analyzed in Tracer; only ESS > 200 values were considered consistent. We used Tree Annotator to produce a maximum clade credibility (MCC) tree from the post-burn-in trees and to determine the 95% probability density of ages for all nodes in the tree. The consensus tree was visualized using FigTree v.1.4.0.

2.4. Morphological analysis

Specimens used in morphological analysis of *Vella pseudocytisus* s.l. included 33 vouchers from GDA, JACA, MA, and SEV herbaria, representing all the taxonomic, cytotypic, and geographical variations of the species (Table S2). Specimens were measured for 9 quantitative traits: leaf length, leaf width, petal length, petal width, sepal length, sepal width, valve (fruit) length, rostrum (fruit) length, and rostrum (fruit) width. These traits were selected according to their diagnostic value in separating intraspecific variations in previous taxonomic studies of this group (Gómez-Campo, 1981, 1993; Crespo et al., 2000; Bañares et al., 2004). Measurements of quantitative traits were taken for each individual specimen using a binocular microscope and a digital caliper (precision of decimal mm). In addition, we examined the hairiness of leaves as a qualitative trait and coded it as 3 binomial factors: glabrousity, hairiness restricted to leaf margin, and hairiness. All subspecies samples were measured for all traits, except those of *glabrata* for variables related to the fruit traits (valve length, rostrum length, rostrum width), because of the lack of ripe fruits in the vouchers.

We analyzed the variation across subspecies and cytotypes of *Vella pseudocytisus* s.l. (4 groups: *glabrata* 2x, *pseudocytisus* 2x, *pseudocytisus* 4x, *paui* 4x) for each morphological trait using general linear models and assessed significant differentiation between pairs of taxa cytotypes with Tukey HSD tests. We conducted a principal coordinate analysis (PCoA) over the data, including 6 quantitative traits, the 3 binomial variables for the qualitative trait, and a principal component analysis (PCA) including only the quantitative variables. Variables related to the fruit traits (valve length, rostrum length, and rostrum width) were excluded from these analyses, given the missing data for *glabrata*.

3. Results

3.1. Plastid and nuclear phylogenetic trees

The *trn*TL sequences rendered a 763-nucleotide (+7 gaps) aligned dataset, and the *trn*LF sequences showed one with 756 nucleotides (+9 gaps). The heuristic parsimony searches found, in both cases, a unique most parsimonious (MP) tree for each analysis, with both trees showing similar topologies. In both cases, 3 poorly to moderately supported monophyletic groups were detected within the *Vella pseudocytisus-V. aspera* complex: i) the *V. aspera* clade, ii) the *pseudocytisus* C Spain range clade, and iii) the *glabrata* clade. Additionally, we found a *paui* Turia range clade in the *trn*TL tree, and a *paui* Alfambra range clade and a *pseudocytisus* SE Spain range clade in the *trn*LF tree (results not shown).

The concatenated plastid *trn*TL + *trn*LF data matrix consisted of 1519 aligned nucleotides and 16 informative gaps. The MP tree (L = 209; CI = 0.866; RI = 0.949; results not shown) and the optimal Bayesian tree (Figure 2A) shared a similar topology. In the optimal Bayesian tree, 5 lineages of the *Vella pseudocytisus-V. aspera* complex were recovered (Figure 2A). The poorly supported *glabrata*/*pseudocytisus* 4x clade collapsed with *V. bourgeana* and *V. spinosa* in a basal polytomy, and the moderately to strongly supported *pseudocytisus* 2x, *paui* Alfambra range, *paui* Turia range, and *V. aspera* lineages collapsed with *V. lucentina* in a more recent (but also poorly supported) polytomy (Figure 2A).

The ITS sequences rendered a 527-nucleotide aligned dataset with no informative indels. The topologies of the MP tree (L = 397; CI = 0.713; RI = 0.926) and the optimal Bayesian trees were highly congruent, and only the last tree will be explained here (Figure 2B). The nuclear tree recovered a strongly supported monophyletic Vellinae, including *Carrichtera* but excluding *Succowia*, and a relatively well-supported (PPS = 0.90) *Vella pseudocytisus-V. aspera* clade. Surprisingly, the subspecies *pseudocytisus* 2x sequences were closer to some *paui* 4x sequences than to their consubspecific *pseudocytisus* 4x sequences. The *glabrata* sequences collapsed with the last lineages in a recent polytomy (Figure 2B).

The combined plastid and nuclear data matrix consisted of 2094 nucleotides and 17 informative indels. The heuristic parsimony search found a unique MP tree (L = 658; CI = 0.737; RI = 0.919), which was congruent with the optimal Bayesian tree shown here (Figure S1; on the journal's website). The cpDNA + ITS tree reconstructed a strongly supported Brassicaceae Lineage II-type (cf. Couvreur et al., 2010) clade. According to this topology, successive strongly supported splits were those of *Succowia*, the poorly supported (Savignyaeae (Zillinae, (Brassiceae, Sisymbrieae))) clade, and the Vellinae clade. Within the more inclusive Vellinae core, a robust sister relationship was reconstructed for the strongly supported *Carrichtera* clade and the weakly supported *Vella* clade. This group showed the successive divergences of *V. spinosa*, *V. bourgeana*, *V. lucentina*/*V. castriliensis*, and the recent polytomy of *V. mairei*, *V. anremerica*, and the *V. pseudocytisus-V. aspera* clade (Figure S1). A moderately supported sister relationship was recovered for the robust *V. aspera* clade and the weak *V. pseudocytisus* clade. Within *V. aspera*, the northwestern Ebro middle valley populations of Castelflorite and Monegrillo diverged from the rest. Within the *V. pseudocytisus* clade, the *paui* 4x Turia range sequences showed a basal paraphyly with respect to the recent polytomy of the *paui* 4x Alfambra range, *pseudocytisus* 2x, and *glabrata* 2x/*pseudocytisus* 4x lineages. In this tree, *pseudocytisus* 4x from central Spain was also reconstructed as sister to the Mahgrebian *glabrata* 2x, but with low support (Figure S1).

3.2. Divergence time estimations

The dated ITS BEAST chronogram (Figure 3) revealed a similar topology to that of the 50% MR consensus Bayesian tree and MP tree (Figure 2). According to this tree, the divergence of *Succowia* from the MRCA of the Brassiceae-Sisymbrieae + Savignyeae + Zilliinae + Vellinae clade was dated to the early Oligocene (Rupelian, 30.5 Ma), the split of the Vellinae (*Carrichtera* plus core Vellinae) in the mid-Miocene (Langhian, 14.7 Ma), and that of the core Vellinae in the late Miocene (Messinian, 7.1 Ma). The *Vella pseudocytisus-V. aspera* lineage was estimated to have diverged in the early Pliocene (4.7 Ma, 95% highest posterior density-HPD-confidence interval, 7.0–2.5 Ma), whereas the splits of *V. pseudocytisus* and *V. aspera* were estimated to have occurred during the transition from the Pliocene to the Pleistocene (2.4 Ma, HPD: 4.2–1.0 Ma and 2.0 Ma, HPD: 4.0–0.5 Ma, respectively). The infraspecific diversification of the *V. pseudocytisus* subspecies and cytotypes spanned the Pleistocene (Figure 3).

3.3. Phenotypic diversity within *Vella pseudocytisus* s.l.

We found significant differences among the 4 subspecies and cytotypes of *Vella pseudocytisus* s.l. for 7 quantitative variables (all except rostrum length and rostrum width; Table S3). According to the Tukey HSD test results, *pseudocytisus* 4x differed significantly from *paui* and *glabrata* in 4 traits and from *pseudocytisus* 2x in 6 traits (Figure 4). On the other hand, there were no significant differences between *pseudocytisus* 2x and *glabrata* 2x in any of the studied quantitative traits, although we could not analyze the fruit variables of the latter taxon. In contrast, the qualitative trait of hairiness of leaves differentiated *pseudocytisus* 2x, with densely hispid leaves, from *glabrata* 2x, with glabrous leaves. Subspecies *paui* 4x was differentiated from the others in having its hairiness restricted exclusively to the leaf margin, while *pseudocytisus* 4x shared its densely hispid leaf character with *pseudocytisus* 2x.

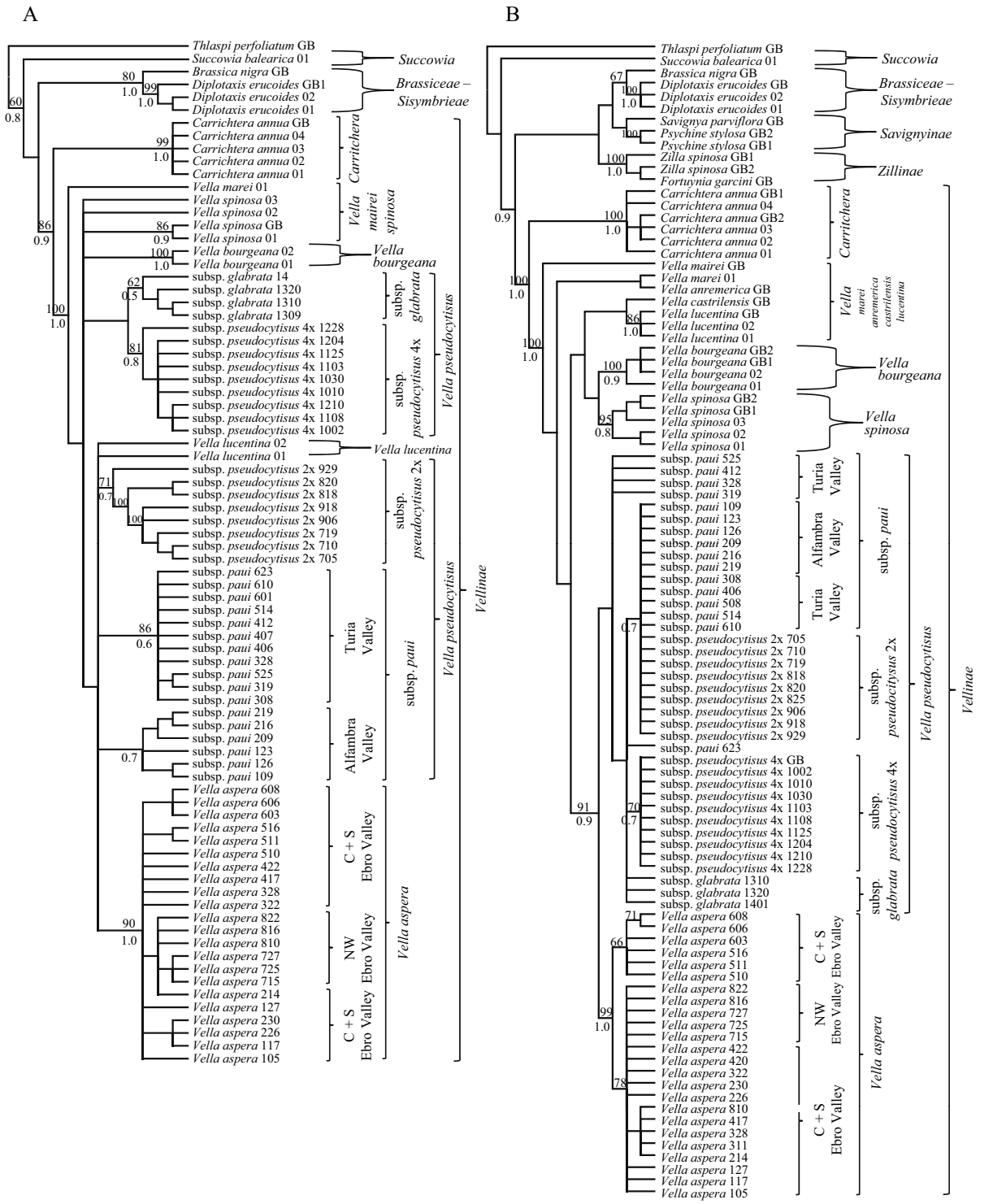

Figure 2. The 50% majority-rule consensus Bayesian trees of the *Vella pseudocytisus*-*V. aspera* complex and related Brassicaceae rooted with *Thlaspi perfoliatum*. **A**- Plastid *trn*TL/LF tree; **B**- Nuclear ITS tree. Bootstrap and posterior probability support values are shown above and below each branch, respectively. Sample codes correspond to source population number + individual number.

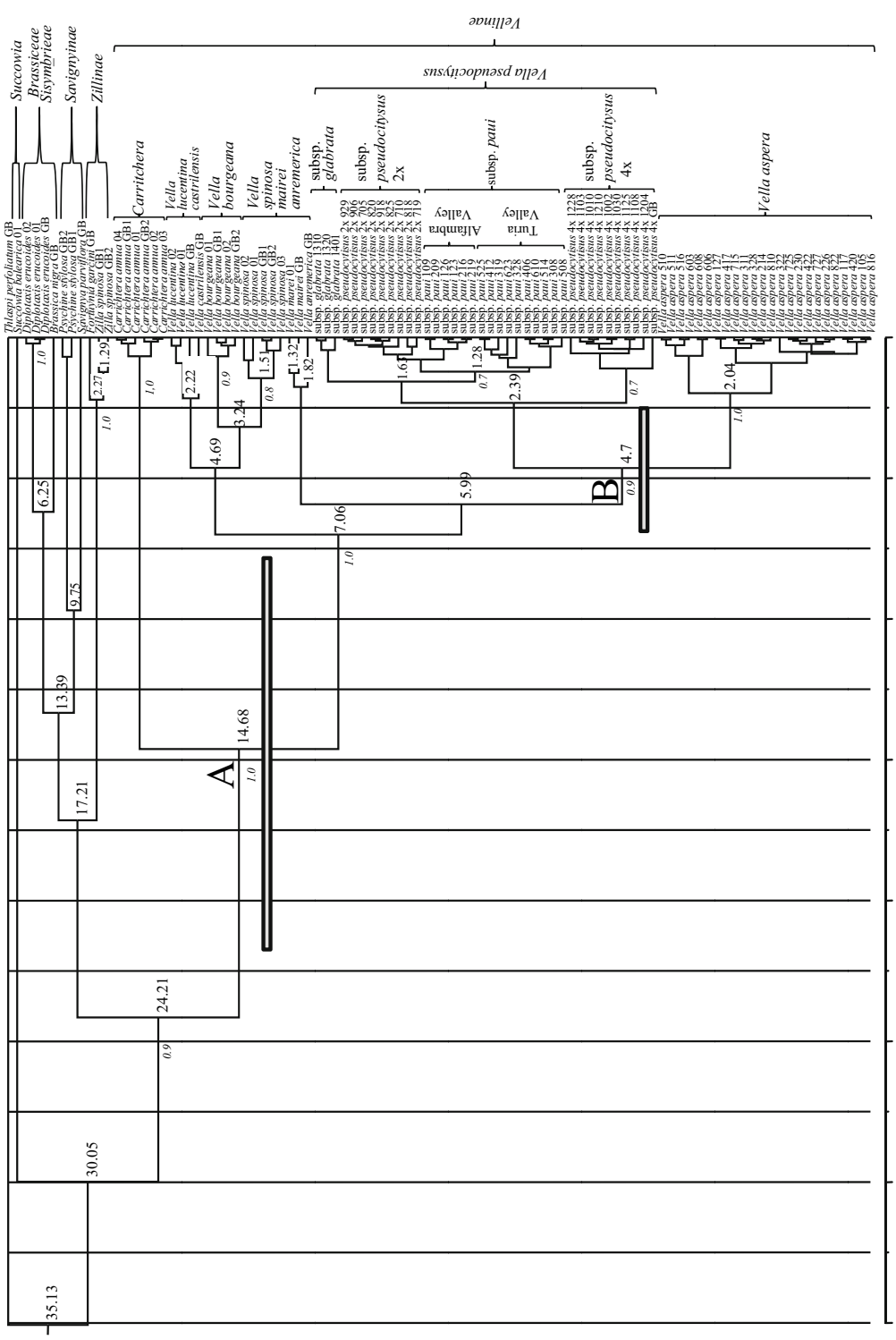

Figure 3. ITS BEAST maximum clade credibility tree of the *Vella pseudocytisus-V. aspera* complex plus the Vellinae and other close Brassicaceae with nodal dating (Ma). Nodes A (crown node of Vellinae) and B (crown node of the *Vella pseudocytisus-V. aspera* complex). Nodal dates were estimated using a lognormal calibration of 30 ± 0.5 Ma for the MRCA of *Thlaspi* and the remaining studied Brassicaceae. Gray bars indicate the confidence intervals of the 2 main nodes. Posterior probability support values are shown below each branch in italics. Sample codes correspond to source population number + individual number.

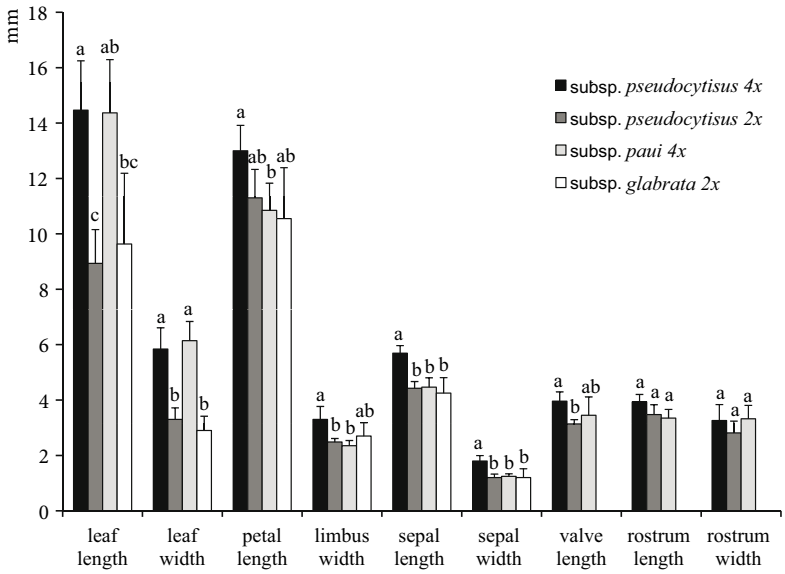

Figure 4. Average values with confidence intervals for 9 quantitative morphological traits measured in 33 herbarium specimens (4 groups, subspecies, and cytotypes) of *Vella pseudocytisus* s.l. (*V. pseudocytisus* subsp. *glabrata* 2x, *pseudocytisus* 2x, *pseudocytisus* 4x, and *paui* 4x). Different letters above bars indicate significant differentiation between pairs of groups for the given trait based on Tukey HSD tests.

The PCA analysis, based on the quantitative traits, differentiated the diploids from the tetraploids (Figure 5). The PCA yielded multiple axes, with the first 3 axes explaining 95.94% of the variance. The first axis (78.02% of variance) separated 2 groups; one included subspecies *pseudocytisus* 4x and *paui* 4x, and the other *pseudocytisus* 2x and *glabrata* 2x. The 2 tetraploids were separated along the second axis (12.65% of variance), but the diploids were not (Figure 5). The joint analysis of both quantitative and qualitative traits in the PCoA also distinguished the tetraploids from the diploids, although with some mixture (results not shown).

4. Discussion

4.1. Evolution of the *Vella pseudocytisus-V. aspera* complex

Our study has contributed to framing the evolutionary history of the *Vella pseudocytisus-V. aspera* complex within the phylogeny of the Vellinae and other related Brassicaceae. Our plastid and nuclear trees show that the *Vella pseudocytisus-V. aspera* clade is one of the most recently evolved Vellinae lineages (Figures 2 and 3), agreeing with the ITS- and morphology-based phylogeny of Crespo et al. (2000). However, our separate and combined cpDNA + ITS analyses have also revealed unexpected relationships resulting from potential past hybridizations among the ancestors of the *Vella pseudocytisus-V. aspera* lineages.

The strong sister relationship of *Carrichtera* to the core Vellinae clade (*V. bourgeana*, *V. pseudocytisus*, and *V. aspera*) is reconstructed from both plastid *trn*TL-LF and nuclear ITS data (Figure 2), supporting the findings of Crespo et al. (2000) and Couvreur et al. (2010). However, the early diverging position of *Succowia*, resolved as sister to the remaining studied taxa in the separate and combined plastid and nuclear MrBayes trees (Figures S1 and S2) and in the combined BEAST tree (Figure 3), raises doubts about its systematic placement. Crespo et al. (2000) classified *Succowia* as the earliest diverging lineage of Vellinae. These authors circumscribed the tribe to the early diverging annual Mediterranean *Succowia* and *Carrichtera* lineages and to the more recently evolved shrubby western Mediterranean *Vella* (and *Euzomodendron*) lineages, based on their relatively well-supported monophyly and their shared morphological fruit traits. Nonetheless, the chromosome base number of the annual monotypic herbs *Succowia* (x = 8) and *Carrichtera* (x = 9) are more similar to those of some Zillinae members (e.g., *Zilla*, *Fortuynia*, *Schouwia*; x = 8) than to that of the core Vellinae woody shrub taxa (x = 17). Crespo et al. (2000) also recognized a poorly supported clade that included the sister Zillinae (x = 8) and Savignyinae (*Psychine*, *Savignia*; x = 15) clades. The family-wide study of Couvreur et al. (2010) separated the Vellinae-Zillinae s.l. group members into 4 independent lineages (*Succowia*, Savignyinae, and the sister Zillinae and Vellinae). Our results (Figures 2, 3, and S1) support this

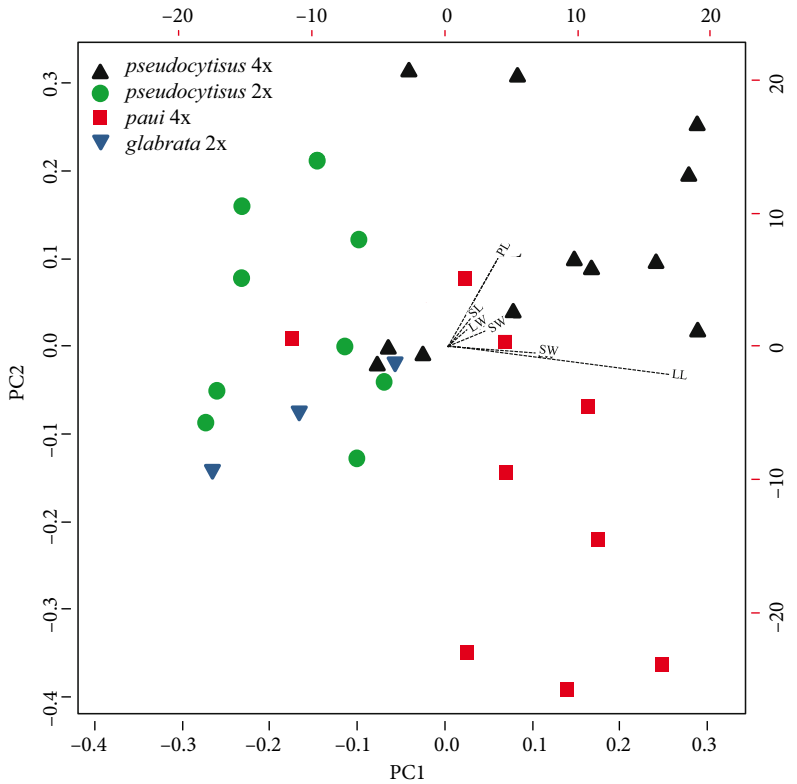

Figure 5. Bidimensional PCA plot of individuals of the 4 subspecies and cytotypes of *Vella pseudocytisus* based on analysis of 6 continuous morphological traits measured on leaves and flowers. LL: leaf length; LW: leaf width; PL: petal length; LW: lamina width; SL: sepal length; SW: sepal width.

conclusion, suggesting a distant relationship of *Succowia* to either Vellinae, Zilliinae, or Savignyinae lineages. According to these results, the isolated *Succowia* should be separated from Vellinae and probably realigned in an independent tribe, whereas *Carrichtera* should be maintained within this tribe based on its strong sister relationship to the remaining core Vellinae taxa. The taxonomic circumscription of the members of other close subtribes should be reanalyzed using a larger sampling of taxa and genes.

The monophyly of the taxa of the core Vellinae group concurs with their shared biological attributes, such as the possession of a woody shrubby habit and early deciduous leaves, probably the result of adaptation to steppe-type Mediterranean climate conditions, and a chromosome base number of x = 17 (Gómez-Campo, 1981). It has been hypothesized that the large chromosome base number of the core Vellinae taxa could have originated from ancient paleoploidization events resulting from genome doubling of crosses between diploid ancestors with lower chromosome base numbers (e.g., x = 9 and x = 8; Gómez-Campo, 1981; Crespo et al., 2000; Pérez-Collazos and Catalán, 2006). Using isozymes, Pérez-Collazos and Catalán (2006) demonstrated the allotetraploid nature of *Vella pseudocytisus* subsp. *paui*, but could not discern between ancient or recent allopolyploidy. However, the existence of a range of diploids, tetraploids, and hexaploids with the same chromosome base number of x = 17 across the core Vellinae taxa suggests the likely occurrence of a diploidization event of ancient paleopolyploids. As the rise of new allopolyploids is a common phenomenon in many angiosperms (i.e. Lowe and Abbot, 1996; Soltis et al., 2004), and the paleopolyploid nature of Brassicaceae and other angiosperms has been well documented (Beilstein et al., 2010; Arias et al., 2014), it is possible that i) the allotetraploid *pseudocytisus* has been derived from the cross between diploid donors of *glabrata* and *pseudocytisus*, ii) the allotetraploid *paui* from the cross of the diploid *V. lucentina* (or a close similar Vellinae taxon) and the diploid *pseudocytisus*, and iii) the allohexaploid *V. aspera* from the cross of diploid *V. lucentina* (or another close Vellinae taxon) and tetraploid *paui* (Figures 2A and 2B). This cross-allopolyploidization scheme would explain the intermediate phylogenetic positions of the hybrid

allopolyploids between their respective parents in the nuclear ITS, the combined cpDNA + ITS trees (Figures 2B, 3, and S1), and the confounding 'apparent' early splits of hexaploid *V. aspera* and tetraploid *V. pseudocytisus* subsp. *paui* from the MRCA of the *Vella pseudocytisus-V. aspera* clade (Figures 2 and 3).

4.2. Divergence, colonization, and speciation patterns within the *Vella pseudocytisus-V. aspera* complex

Dated molecular phylogenies are crucial to understanding the diversification rates of the lineages with respect to historical events such as colonization, hybridization, and speciation processes within particular geographical settings (Renner, 2005; Arias et al., 2014). The western Mediterranean region is one of the major hotspots of angiosperm diversity in the northern hemisphere (Médail and Diadema, 2009). A conjunction of paleogeographic and paleoclimatic events concurred in the western Mediterranean across the late Tertiary and the Quaternary, creating multiple historical scenarios for the origin of its rich flora. A series of microplate tectonics during the Miocene (Meulenkamp and Sissingh, 2003) caused marine transgressions and regressions that successively isolated and connected NW Africa and the Iberian Peninsula (Krijgsman, 2002), allowing lineage dispersal and concomitant allopatric speciation events in several Ibero-Mahgrebian plant lineages (Lavergne et al., 2013). The climate changes related to the Messinian salinity crisis (6 Ma; Suc, 1984), the onset of the Mediterranean climate (3.5 Ma; Suc, 1984), and the Pleistocene glaciations (2.0 Ma; Bertoldi et al., 1989; Combourieu-Nebout, 1993) acted as selective filters for plant survival but also created new conditions for plant speciation, such as the numerous Ibero-Mahgrebian glacial refugia and the hybrid zones where secondary contacts among previously isolated species fostered hybridization and polyploidization events during the interglacial and postglacial phases (Barton and Hewitt, 1989).

The *Vella pseudocytisus-V. aspera* complex reflects a diversity of speciation processes linked to the changing environment of the Ibero-Mahgrebian region during the late Tertiary-Quaternary. The origin of the group is reconstructed between the Tortonian (stem node, 11.6 Ma) and the Messinian (crown node, 7.1 Ma) in the late Miocene (Figure 3).

During the Tortonian period (12–9 Ma), the western Mediterranean area consisted of the North African platform, which included the High and Middle Atlas ranges, the subcoastal Tell-Atlas range, and a large Betic-Rifian range island, separated from northwestern Africa and the proto-Iberian Peninsula by the Rifian and Betic marine corridors, respectively (Krijgsman, 2002). The closure of these corridors between the late Tortonian and mid-Messinian (Rosenbaum et al., 2002) created a land bridge between NW Africa and S Europe, which acted as a main dispersal route for the African and European biotas (Rodríguez-Sánchez et al., 2008). The opening of the Gibraltar Strait at the end of the Miocene (5.3 Ma) broke up the terrestrial connection between the African and European (Iberian) platforms (Rosenbaum et al., 2002; Loget and Van den Driessche, 2006), fostering isolation-by-distance (IBD) speciation processes on both sides of the strait (Rodríguez-Sánchez et al., 2008). It could be hypothesized that the presumably oldest diploid descendant lineages of the MRCA of the *Vella pseudocytisus-V. aspera* clade diverged in the Mahgrebian-Betic range at the end of the Miocene (Figure 3). The current distributions of the extant diploid representatives of the group (*glabrata* 2x in the Middle and Tell-Atlas ranges and *pseudocytisus* 2x in the Betic range, Figure 1) suggest that the 2 diploid taxa speciated by IBD divergence after the subsidence of the Gibraltar Strait.

The artifactual reconstruction of the allopolyploids *V. aspera* 6x and *paui* 4x as the earliest splitting lineages of the group (Figures 2 and 3) could not mask their secondary derived origins from crosses and genome duplications of more ancient diploid and low polyploid lineages (Figure S1). Allopolyploids and hybrid taxa that occupy artificial intermediate positions in nuclear gene-based phylogenies should be discarded from dating and biogeographical analyses due to the distortion caused to the estimates (Pimentel et al., 2013; Inda et al., 2014). However, alternative interpretations should be evaluated for those groups formed (almost) exclusively by allopolyploid lineages. Our cpDNA + ITS chronogram dated the divergences of *V. pseudocytisus* (2.4 Ma) and *V. aspera* (2.0 Ma) to the boundary between the Pliocene and the Pleistocene (Figure 3). All the colonization and hybridization events that resulted in the current distribution of the extant polyploid lineages of the complex probably occurred in the timespan elapsed since the splits of the MRCA of the group and the species' crown nodes. According to the hybridization scheme suggested by the cpDNA and ITS data (Figure S1) and the dated phylogeny (Figure 3), a potential long-distance dispersal of a southern Spanish endemic Vellinae diploid lineage and the Betic *pseudocytisus* 2x lineage to the NE Spain Teruel range, followed by hybrid allopolyploidization, occurred in the late Pliocene (4.7–2.8 Ma), creating the tetraploid *V. pseudocytisus* subsp. *paui*. This was probably concomitant with a potential parallel long-distance dispersal of the diploid Mahgrebian *glabrata* and the Betic *pseudocytisus* 2x lineages to the central Iberian range (2.5 Ma), originating the allotetraploid *V. pseudocytisus* subsp. *pseudocytisus* 4x after crossing and whole-genome duplication (WGD). The origin of allohexaploid *Vella aspera* in the late Pliocene to early Pleistocene (4.7–2.0 Ma) could be explained by

a potential long-distance dispersal of a southern Spain endemic Vellinae diploid lineage and a potential short-distance dispersal of the NE Spain tetraploid *paui* 4x to the NE Spain middle Ebro Valley, followed by crossing and WGD.

The climatic and geomorphological changes of the Iberian Peninsula during the Messinian-Pliocene transition support the suggested dispersal and the rise of the new polyploid taxa in their geographical settings. The dissecation of an inland sea and its opening to the Mediterranean created the Ebro River valley basin, a gypsum-rich steppe area dominated by a continental dry climate since the Pliocene (Pérez-Collazos and Catalán, 2006; Pérez-Collazos et al., 2008). The onset of the Mediterranean climate also created dry continental steppe niches in the high inland plateaus of the Atlas and the central and NE Iberian ranges. Almost all the intraspecific and intracytotypic diversifications of the 5 *Vella pseudocytisus-V. aspera* lineages occurred in the Pleistocene (Figure 3). The glacial phases affected the northern and southern Ibero-Mahgrebian ranges and neighboring areas differently. A larger number of glacial refugia have been identified/proposed in the warm Mahgrebian and southern Iberian area than in the cold northern Iberian area (Médail and Diadema, 2009), a fact that is reflected in the higher number of plant endemisms occurring in the south (Rodríguez-Sánchez et al., 2008). Though most of the northern Iberian *V. pseudocytisus* and *V. aspera* populations are distributed today at altitudes below the estimated distributions of the Pleistocene ice caps, they were probably affected by a severe, cold climate, which probably caused important population bottlenecks (Pérez-Collazos and Catalán, 2006). According to this scenario, it might be plausible that only the better adapted polyploids survived the Quaternary glacial ages in the north, whereas the less adapted diploids were sheltered in the warm refuges of the south, resulting in the present distribution of taxa and cytotypes (Figure 1).

4.3. Systematics of the *Vella pseudocytisus–V. aspera* complex taxa

4.3.1 *Vella aspera*

Although systematic and evolutionary studies of the Brassicaceae and the Vellinae had been accomplished using morphological and molecular data (Warwick and Black, 1994; Crespo et al., 2000; Koch, 2003; Warwick and Sauder, 2005; Crespo et al., 2005), little detailed research had been conducted on the *Vella pseudocytisus-V. aspera* complex. The inclusion of *Boleum* in *Vella* has been proposed by several authors since its original description by Persoon (*Vella aspera*; 1806). Warwick and Al-Shehbaz (1998) and Al-Shehbaz (2012) supported this treatment based on their shared morphological traits such as woody habit, fusion of paired inner filaments, possession of short pedicels, saccate lateral sepals, long petal claws, dark-veined petal blades, seedless flattened beaks, 3 or 5 strongly veined valves, and acutely notched cotyledons. All these characters justify the inclusion of *Boleum* in *Vella* rather than their taxonomical separation based on the short pedicellate, indehiscent, sessile fruits of *Boleum* and the long pedicellate, dehiscent, gynophorate, or sessile fruits of *Vella*. Warwick and Black (1994), using DNA restriction site variation, supported the classification of both *V. aspera* (*Boleum*) and *V. bourgeana* (*Euzomodendron*) within *Vella*. Ponce-Díaz (1997, unpublished PhD dissertation) and Ponce-Díaz et al. (1999) found a close genetic relationship of *V. aspera* to *Carrichtera* using allozymes, but a closer one to *V. pseudocytisus* and *V. bourgeana* using ISSRs. Crespo et al. (2000), based on ITS and morphological data, also subsumed *V. aspera* within *Vella*, but recognized the sister *Euzomodendron* (*V. bourgeana*) as an independent genus.

In agreement with Persoon (1806), Warwick and Al-Shehbaz (1998), and Al-Shehbaz (2012), our results support the alignment of *Boleum* within *Vella* (*V. aspera* Persoon), since our plastid and nuclear phylogenetic trees reconstruct *Vella aspera* as the sister taxon of the *V. pseudocytisus* clade (Figures 2, 3, and S1). Our data also support the alignment of *Euzomodendron bourgaeanum* within *Vella* (*V. bourgeana* (Cosson) Warwick and Al-Shehbaz) based on its reconstruction as a sister group of *V. spinosa* (Figures 2, 3, and S1).

4.3.2. *Vella pseudocytisus* assemblage: subspecies *pseudocytisus, glabrata, paui,* and *orcensis*

Our plastid and nuclear phylogenetic analyses have identified 4 lineages within *Vella pseudocytisus* s.l. (Figures 2 and ,3): i) Mahgrebian *glabrata* 2x; ii) NE Spain *paui* 4x (Alfambra and Turia ranges, respectively); iii) C Spain *pseudocytisus* 4x; and iv) SE Spain *pseudocytisus* 2x. These lineages show a narrow geographical distribution, a specific ploidy level, and a past history of dispersals and allopatric speciations coupled with allopolyploidization events.

The cytotypic and evolutionary traits of these lineages are also matched with specific morphological traits. The statistical analysis of quantitative traits showed that the combination of 6 leaf and floral characters significantly discriminates the 4 taxa and cytotypes (Figure 4). Similarly, the PCA analysis separated 3 of the 4 groups in the morphospace defined by the first 2 axes (Figure 5). The analysis of the qualitative hairiness trait allowed us to differentiate the 3 previously recognized subspecies (including the 2 groups that were not distinguished according to the quantitative traits, *pseudocytisus* 2x and *glabrata*). Although there were no differences between the 2 disjunct geographical cytotypes of *Vella pseudocytisus* subsp. *pseudocytisus* in the hairiness of leaves, their recognition as independent taxa is supported by their

quantitative morphological differences revealed in our phenotypic study (Figures 4 and 5) and in previous studies (Blanca et al., 1999), the evolutionary divergence detected between them (Figures 2 and 3), their different ploidy levels (2n = 2x = 34 and 2n = 4x = 68 in the SE Spain and C Spain ranges, respectively; Figure 1), and their likely long-term isolation caused by the polyploidization barrier and the geographical distance that separates them (400 km; Figure 1). Furthermore, the cpDNA + ITS patristic distances observed among the core Vellinae lineages (Figure S1) support the recognition of the 2 lineages of *Vella pseudocytisus* subsp. *pseudocytisus* as independent subspecies. Accordingly, we describe the specimens (individuals) from the Betic range as *Vella pseudocytisus* subsp. *orcensis* Vivero, Simón-Porcar, Pérez-Collazos, & Catalán (subsp. nov.).

Vella pseudocytisus subsp. *orcensis* Vivero, Simón-Porcar, Pérez-Collazos, & Catalán (subsp. nov.)

Typus: Spain. Granada: Collected on gypsum substrate in Venta Micena near Orce (Granada). Coordinates: 37°44′06.33″N, 2°23′31.19″W; 970 m a.s.l. 21/05/2004. Collector: Pilar Catalán, vouchered as JACA R296885 (holotype: JACA R296882; isotypes: GDA22576; GDA42088; GDA30910; MA45978).

Description: Spineless multibranched shrub, up to 100 cm high, hispid with simple setae. Oblong-lanceolate persistent, simple leaves, 8.0–10 × 3.0–4.0 mm, densely covered with short appressed hairs. Ebracteate and raceme inflorescence with 15–30 flowers on top of short peduncles. Petals 10–12 mm long; suborbicular lamina 2.0–3.0 mm wide, yellow and finally whitish; claw filiform protruding overtopping calyx. Hispid and erect sepals, 2.0–3.0 × 1.0–1.5 mm. Erect silicules, 1(–2) seeded; bilocular and dehiscent at the base, approx. 3.0 mm in length, with hispid valves, glabrous rostrum, equal or slightly longer than the base, 3.0–4.0 × 2.5–3.5 mm. 2n = 2x = 34. Flowering in April–May, fruiting in June–July.

Etymology: The name of the subspecies *orcensis* refers to the name of the type locality (Orce).

Ecology: The subspecies individuals are dominant in open steppe shrublands with *Stipa tenacissima*, *Helianthemum squamatum*, *Lepidium subulatum*, *Ononis tridentata*, and *O. fruticosa*. The plant grows in disturbed areas, on calcareous or gypsum substrates at altitudes between 900 and 1200 m.

Key to subspecies of *Vella pseudocytisus* (Gómez-Campo, 1981; Crespo, 1992; current study):

1. Densely hairy leaves 2
1. Glabrescent leaves 3
2. Leaves ≥12 mm length and 5 mm width; sepals ≥5 mm length and 1.5 mm width; limbus ≥3 mm width; valve length ≥3.5 mm ..... subsp. *pseudocytisus* L.
2. Leaves ≤12 mm length and 4 mm width; sepals ≤5 mm length and 1.5 mm width; limbus ≤3 mm width; valve length ≤3.5 mm ..... subsp. *orcensis* Vivero et al.
3. Hairs only at the edge of the leaf ..... subsp. *paui* Gómez-Campo
3. Hairs on both surfaces of leaf ..... subsp. *glabrata* Greuter

Acknowledgments

The authors thank Teresa Garnatje, Joan Vallès, and José Gabriel Segarra-Moragues for supplying some plant materials; the INIA germplasm bank for providing seeds of *Vella pseudocytisus* subsp. *glabrata*; the curators of the GDA, JACA, MA, and SEV herbaria for the loaning of vouchers; and Emily Lemonds and Douglas Laing for linguistic assistance. This work was supported by a Spanish Aragón Government research grant project (P2002/0290) and by Spanish Aragón Government and European Social Fund co-funding support to the Bioflora research group.

References

Al-Shehbaz IA (2012). A generic and tribal synopsis of the Brassicaceae (Cruciferae). Taxon 61: 931–954.

Arias T, Beilstein MA, Tang M, McKain MR, Pires JC (2014). Diversification time among Brassica (Brassicaceae) crops suggest hybrid formation after 20 million years of divergence. Am J Bot 101: 86–91.

Baldwin BG, Sanderson MJ, Porter JM, Wojciechowski MF, Campbell CS, Donoghue MJ (1995). The ITS region of nuclear ribosomal DNA: a valuable source of evidence on angiosperm phylogeny. Ann Mo Bot Gard 82: 247–277.

Bañares Á, Blanca G, Güemes J, Moreno JC, Ortiz S (2004). Atlas y Libro Rojo de la Flora Vascular Amenazada de España. Madrid, Spain: Dirección General de Conservación de la Naturaleza (in Spanish).

Barton NH, Hewitt GM (1989). Adaptation, speciation and hybrid zones. Nature 341: 497–503.

Beilstein MA, Al-Shehbaz IA, Mathews S, Kellogg EA (2008). Brassicaceae phylogeny inferred from phytochrome A and *ndh*F sequence data: tribes and trichomes revisited. Am J Bot 95: 1307–1327.

Beilstein MA, Nagalingum NS, Clements MD, Manchester SR, Mathews S (2010). Dated molecular phylogenies indicate a Miocene origin for *Arabidopsis thaliana*. P Natl Acad Sci USA 107: 18724–18728.

Bertoldi R, Rio D, Thunell R (1989). Pliocene-Pleistocene vegetational and climatic evolution of the south-central Mediterranean. Palaeogeogr Palaeocl 72: 263–275.

Blanca G, Cabezudo B, Fernández-Bermejo JE, Herrera CM, Molera-Mesa J, Muñoz J, Valdés B (1999). Libro rojo de flora silvestre amenazada de Andalucía. Tomo I. Especies en peligro de extinción. Seville, Spain: Consejería de Medio Ambiente, Junta de Andalucía. (in Spanish).

Combourieu-Nebout N (1993). Vegetation response to Upper Pliocene glacial/interglacial cyclicity in the Central Mediterranean. Quaternary Res 40: 228–236.

Couvreur TLP, Franzke A, Al-Shehbaz IA, Bakker FT, Koch MA, Mummenhoff K (2010). Molecular phylogenetics, temporal diversification, and principles of evolution in the mustard family (Brassicaceae). Mol Biol Evol 27: 55–71.

Crespo MB (1992). A new species of *Vella* L. (Brassicaceae) from the south-eastern part of the Iberian Peninsula. Bot J Linn Soc 109: 369–376.

Crespo MB, Lledó MD, Fay MF, Chase MW (2000). Subtribe Vellinae (Brassiceae, Brassicaceae): a combined analysis of ITS nrDNA sequences and morphological data. Ann Bot-London 86: 53–62.

Crespo MB, Ríos S, Vivero JL, Prados J, Hernández-Bermejo E, Lledó MD (2005). A new spineless species of *Vella* (Brassicaceae) from the high mountains of south-eastern Spain. Bot J Linn Soc 149: 121–128.

Darriba D, Taboada GL, Doallo R, Posada D (2012). jModelTest 2: more models, new heuristics and parallel computing. Nat Methods 9: 772.

Doyle JJ, Doyle JL (1990). Isolation of plant DNA from fresh tissue. Focus 12: 13–15.

Drummond AJ, Rambaut A (2007). BEAST: Bayesian evolutionary analysis by sampling trees. BMC Evol Biol 7: 214.

Gandolfo MA, Nixon KC, Crepet WL, Ratcliffe GE (1997). A new fossil fern assignable to Gleicheniaceae from late cretaceous sediments of New Jersey. Am J Bot 84: 483–493.

Gómez-Campo C (1981). Taxonomic and evolutionary relationships in the genus *Vella* L. (Cruciferae). Bot J Linn Soc 82: 165–179.

Gómez-Campo C (1993). *Vella* L. In: Castroviejo S, Aedo C, Gómez-Campo C, Lainz M, Montserrat P, Morales R, Muñoz-Garmedia F, Nieto-Feliner G, Rico E, Talavera S et al., editors. Flora Ibérica. Plantas Vasculares de la Península Ibérica e Islas Baleares. Vol. IV (Cruciferae-Monotropaceae). 1st ed. Madrid, Spain: Real Jardín Botánico, pp. 414–417 (in Spanish).

Guindon S, Gascuel O (2003). A simple, fast, and accurate method to estimate large phylogenies by maximum likelihood. Systematic Biol 52: 696–704.

Guzmán D, Goñi M, García MB (2000). Estudio y conservación de seis especies de flora amenazada en Aragón, LIFE 1997 - 2000. Zaragoza, Spain: Diputación General de Aragón (in Spanish).

Huelsenbeck JP, Ronquist F (2001). MRBayes: Bayesian inference of phylogenetic trees. Bioinformatics 17: 754–755.

Inda LA, Sanmartin I, Buerki S, Catalán P (2014). Mediterranean origin and Miocene-Holocene Old World diversification of meadow fescues and ryegrasses (*Festuca* subgenus *Schedonorus* and *Lolium*). J Biogeogr 41: 600–614.

Janchen E (1942). Das System der Cruciferen. Österr Bot Z 91: 1–21 (in German).

Jiménez JF, Sánchez-Gómez P, Güemes J, Rosselló JA (2005). Phylogeny of snapdragon species (*Antirrhinum*; Scrophulariaceae) using non-coding cpDNA sequences. Isr J Plant Sci 53: 47–54.

Koch MA (2003). Molecular phylogenetics, evolution and population biology in Brassicaceae. In: Sharma AK, Sharma A, editors. Plant Genome: Biodiversity and Evolution, Vol. 1a. 1st ed. Enfield, UK: Science Publishers, pp. 1–35.

Krijgsman W (2002). The Mediterranean: *Mare Nostrum* of Earth sciences. Earth Planet Sc Lett 205: 1–12.

Lavergne S, Hampe A, Arroyo J (2013). In and out of Africa: how did the Strait of Gibraltar affect plant species migration and local diversification? J Biogeogr 40: 24–36.

Leaché AD, Reeder TW (2002). Molecular systematics of the Eastern Fence Lizard (*Sceloporus undulatus*): a comparison of parsimony, likelihood, and Bayesian approaches. Systems Biol 51: 44–68.

Loget N, Van den Driessche J (2006). On the origin of the Strait of Gibraltar. Sediment Geol 188: 341–356.

Lowe AJ, Abbott RJ (1996). Origins of the new allopolyploid species *Senecio cambrensis* (Asteraceae) and its relationship to the Canary Islands endemic *Senecio teneriffae*. Am J Bot 83: 1365–1372.

Médail F, Diadema K (2009). Glacial refugia influence plant diversity patterns in the Mediterranean Basin. J Biogeogr 36: 1333–1345.

Meulenkamp JE, Sissingh W (2003). Tertiary palaeogeography and tectonostratigraphic evolution of the Northern and Southern Peri-Tethys platforms and the intermediate domains of the African–Eurasian convergent plate boundary zone. Palaeogeogr Palaeocl 196: 209–228.

Muller J (1981). Fossil pollen records of extant angiosperms. Bot Rev 47: 1–142.

Pérez-Collazos E, Catalán P (2006). Palaeopolyploidy, spatial structure and conservation genetics of the narrow steppe plant *Vella pseudocytisus* subsp. *paui* (Vellinae, Cruciferae). Ann Bot-London 97: 635–647.

Pérez-Collazos E, Segarra-Moragues JG, Catalán P (2008). Two approaches for the selection of Relevant Genetic Units for Conservation in the narrow European endemic steppe plant *Boleum asperum* (Brassicaceae). Biol J Linn Soc 94: 341–354.

Persoon CH (1806). Synopsis Plantarum, Vol. 2. Paris, France: C.F. Cramerum.

Pimentel M, Sahuquillo E, Torrecilla Z, Popp M, Catalán P, Brochmann C (2013). Hybridizations and long-distance colonization at different time scales: towards resolution of long-term controversies in the sweet vernal grasses (*Anthoxanthum*). Ann Bot-London 112: 1015–1030.

Ponce-Díaz P, Zwart JL, Martín JP, Sánchez-Yélamo MD (1999). A preliminary consideration about species relationships in *Vellinae* and *Savignyinae* (Cruciferae). Cruciferae Newslett 21: 23–24.

Renner SS (2005). Relaxed molecular clocks for dating historical plant dispersal events. Trends 10: 550–558.

Rodríguez-Sánchez F, Pérez-Barrales R, Ojeda F, Vargas P, Arroyo J (2008). The Strait of Gibraltar as a melting pot for plant biodiversity. Quaternary Sci Rev 27: 2100–2117.

Rosenbaum G, Lister GS, Duboz C (2002). Reconstruction of the tectonic evolution of the western Mediterranean since the Oligocene. J Virtual Explor 8: 107–130.

Soltis DE, Soltis PS, Pires JC, Kovarik A, Tate JA, Mavrodiev E (2004) Recent and recurrent polyploidy in *Tragopogon* (Asteraceae): cytogenetic, genomic, and genetic comparisons. Biol J Linn Soc 82: 485–501.

Suc JP (1984). Origin and evolution of the Mediterranean vegetation and climate in Europe. Nature 307: 429–432.

Swofford DL (2002). PAUP*: Phylogenetic Analysis Using Parsimony (*and Other Methods). Sunderland, MA, USA: Sinauer Associates.

Taberlet P, Gielly L, Pautou G, Bouvet J (1991). Universal primers for amplification of three non-coding regions of chloroplast DNA. Plant Mol Biol 17: 1105–1109.

Tamura K, Peterson D, Peterson N, Stecher G, Nei M, Kumar S (2011). MEGA5: Molecular Evolutionary Genetics Analysis using maximum likelihood, evolutionary distance, and maximum parsimony methods. Mol Biol Evol 28: 2731–2739.

Warwick SI, Al-Shehbaz IA (1998). Generic evaluation of *Boleum*, *Euzomodendron* and *Vella* (Brassicaceae). Novon 8: 321–325.

Warwick SI, Black LD (1994). Evaluation of the subtribes Moricandiinae, Savignyinae, Vellinae and Zillinae (Brassicaceae, tribe Brassiceae) using chloroplast DNA restriction site variation. Can J Bot 72: 1692–1701.

Warwick SI, Francis A, Al-Shehbaz IA (2006). Brassicaceae: species checklist and database on CD-Rom. Plant Syst Evol 259: 249–258.

Warwick SI, Sauder CA (2005). Phylogeny of tribe Brassiceae (Brassicaceae) based on chloroplast restriction site polymorphisms and nuclear ribosomal internal transcribed spacer and chloroplast *trn*L intron sequences. Can J Bot 83: 467–483.

White TJ, Bruns T, Lee S, Taylor J (1990). Amplification and direct sequencing of fungal ribosomal RNA genes for phylogenetics. In: Innis MA, Gelfand DH, Sninsky JJ, White TJ, editors. PCR Protocols: A Guide to Methods and Applications. 1st ed. New York, NY, USA: Academic Press, pp. 315–322.

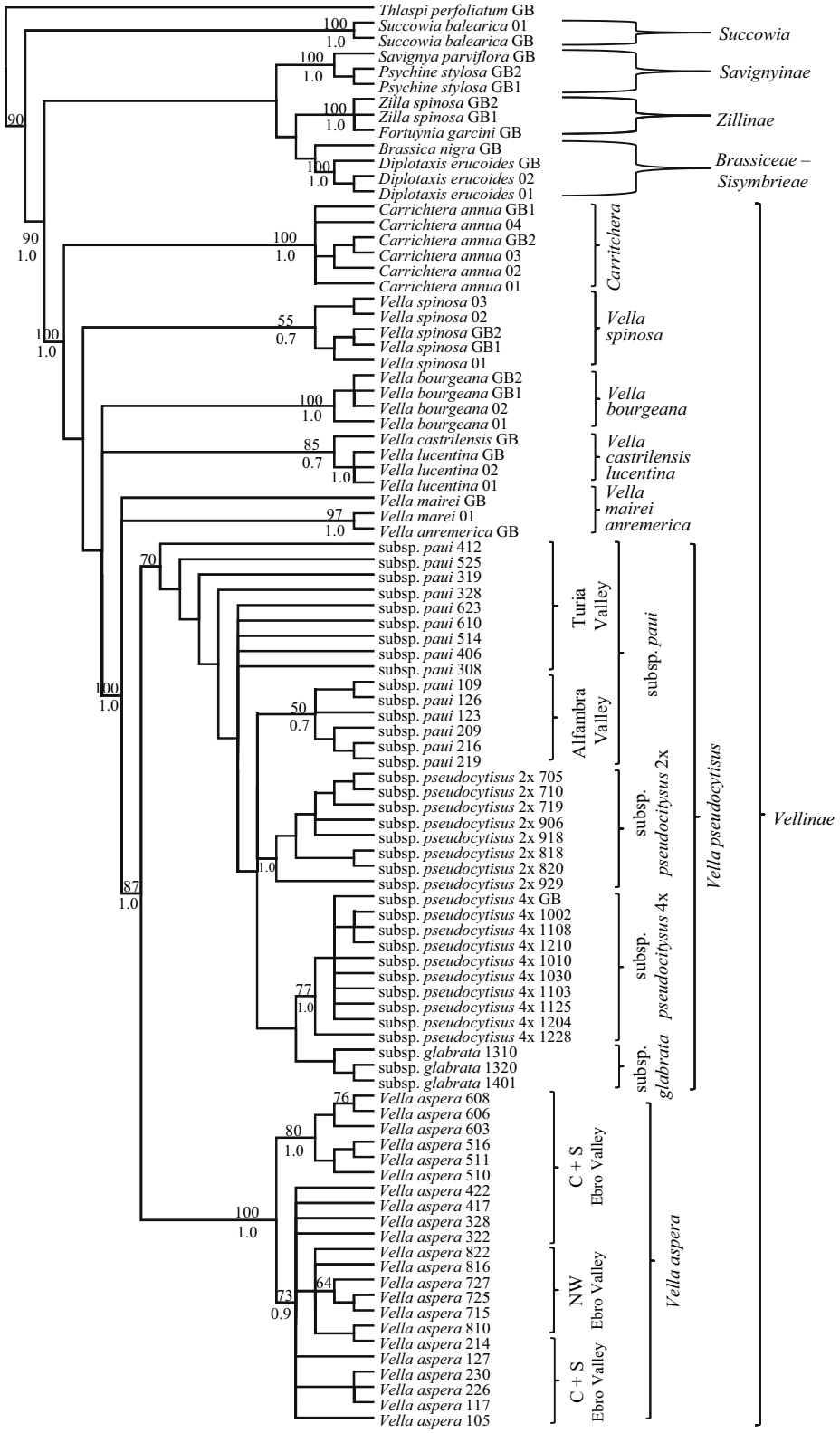

Figure S1. Combined cpDNA + ITS 50% MR consensus Bayesian tree of the *Vella pseudocytisus-V. aspera* complex and outgroup taxa rooted with *Thlaspi perfoliatum*. Bootstrap and posterior probability support values are shown above and below each branch, respectively. Sample codes correspond to source population number + individual number.

Table S1. Additional DNA sequences from 15 taxa, downloaded from GenBank and included in the phylogenetic analyses.

Species	ITS	*trn*TL	*trn*LF
Brassica nigra	GQ268057	AF451579	AF451578
Carrichtera annua	AF263386; DQ248929	--	AY751761
Diplotaxis erucoides	AF263401	--	DQ984088
Euzomodendron bourgeanum	AF263385; AY722496	--	--
Fortuynia garcini	AF263398	--	--
Psychine stylosa	AF263403; DQ248935	--	--
Savignya parviflora subsp. *parviflora*	AF263399	--	--
Thlaspi perfoliatum	AY154810	--	AY154787
Vella anremerica	AF263387	--	--
Vella castrilensis	AJ841702	--	--
Vella lucentina	AF263389	--	--
Vella mairei	AF263388	--	--
Vella spinosa	AF263390; DQ249833	--	AY751773
Zilla spinosa	AF263397; AY722501	--	--
Vella pseudocytisus subsp. *pseudocytisus*	--	--	AF263393

Table S2. Specimens used in the morphological analysis of *Vella pseudocytisus* s.l. representing all the taxonomic, cytotypic, and geographical variation of the species.

Num.	Vella *pseudocytisus* subspecies	Herbarium	Code
1	subsp. *glabrata* 2x	GDA	GDA57390
2	subsp. *glabrata* 2x	MA	MA45976
3	subsp. *glabrata* 2x	MA	MA521224
4	subsp. *pseudocytisus* 2x	GDA	GDA22576
5	subsp. *pseudocytisus* 2x	GDA	GDA30910
6	subsp. *pseudocytisus* 2x	GDA	GDA42088
7	subsp. *pseudocytisus* 2x	JACA	JACA R296882
8	subsp. *pseudocytisus* 2x	JACA	JACA R296883
9	subsp. *pseudocytisus* 2x	JACA	JACA R296884
10	subsp. *pseudocytisus* 2x	JACA	JACA R296885
11	subsp. *pseudocytisus* 2x	JACA	JACA R296886
12	subsp. *pseudocytisus* 2x	MA	MA45978
13	subsp. *paui* 4x	JACA	JACA R296887
14	subsp. *paui* 4x	JACA	JACA R296888
15	subsp. *paui* 4x	MA	MA428045
16	subsp. *paui* 4x	MA	MA440498
17	subsp. *paui* 4x	MA	MA45989
18	subsp. *paui* 4x	MA	MA614862
19	subsp. *paui* 4x	MA	MA794197
20	subsp. *paui* 4x	SEV	SEV218673
21	subsp. *paui* 4x	SEV	SEV218674
22	subsp. *pseudocytisus* 4x	JACA	JACA R296889
23	subsp. *pseudocytisus* 4x	JACA	JACA R296890
24	subsp. *pseudocytisus* 4x	JACA	JACA R296891
25	subsp. *pseudocytisus* 4x	SEV	SEV112968
26	subsp. *pseudocytisus* 4x	SEV	SEV119353
27	subsp. *pseudocytisus* 4x	SEV	SEV260674
28	subsp. *pseudocytisus* 4x	SEV	SEV28321
29	subsp. *pseudocytisus* 4x	SEV	SEV3278
30	subsp. *pseudocytisus* 4x	SEV	SEV60050
31	subsp. *pseudocytisus* 4x	SEV	SEV60355
32	subsp. *pseudocytisus* 4x	SEV	SEV7668
33	subsp. *pseudocytisus* 4x	SEV	SEV92967

Table S3. Average ± SD values of 9 quantitative traits measured in 33 herbarium specimens of subspecies and cytotypes of *Vella pseudocytisus* (4 groups: *V. pseudocytisus* subsp. *glabrata* 2x, *pseudocytisus* 2x, *pseudocytisus* 4x, *paui* 4x). F-values and their associated P-values were obtained from a general linear model testing of differences among subspecies and cytotypes (4 groups) for each trait. N: sampling size; na: data not available. Significance: ***: P < 0.001; **: P < 0.01; *: P < 0.05; ns: nonsignificant.

	subsp. *pseudocytisus* 4x (N = 12)	subsp. *pseudocytisus* 2x (N = 9)	subsp. *paui* 4x (N = 9)	subsp. *glabrata* 2x (N = 3)	F-value	P-value
Leaf length (mm)	14.5 ± 3.1	8.9 ± 1.9	14.4 ± 2.9	9.6 ± 2.3	9.68	0.000***
Leaf width (mm)	5.8 ± 1.4	3.3 ± 0.6	6.1 ± 1.1	2.9 ± 0.5	17.45	0.001***
Petal length (mm)	13.0 ± 1.6	11.3 ± 1.6	10.9 ± 1.5	10.6 ± 1.6	3.74	0.024*
Lamina width (mm)	3.3 ± 0.8	2.5 ± 0.2	2.4 ± 0.3	2.7 ± 0.4	5.11	0.007**
Sepal length (mm)	5.7 ± 0.5	4.4 ± 0.4	4.5 ± 0.5	4.3 ± 0.5	16.97	0.000***
Sepal width (mm)	1.8 ± 0.3	1.2 ± 0.2	1.2 ± 0.1	1.2 ± 0.3	11.80	0.046***
Valve length (mm)	4.0 ± 0.6	3.1 ± 0.2	3.5 ± 1.0	na	4.39	0.027*
Rostrum length (mm)	3.9 ± 0.5	3.5 ± 0.5	3.4 ± 0.5	na	2.70	0.093 ns
Rostrum width (mm)	3.3 ± 1.0	2.8 ± 0.7	3.3 ± 0.7	na	0.76	0.483 ns